

Local mode behaviour in quasi-1D CDW systems

H. Fehske^a, G. Wellein^b, H. Büttner^a, A. R. Bishop^c, and M. I. Salkola^d

^aPhysikalisches Institut, Universität Bayreuth, D-95440 Bayreuth, Germany

^bRegionales Rechenzentrum Erlangen, Universität Erlangen, 91058 Erlangen, Germany

^cMSB262, Los Alamos National Laboratory, Los Alamos, NM 87545, USA

^dSuperconductor Technologies Inc., Santa Barbara, CA 93111, USA

Abstract

We analyze numerically the ground-state and spectral properties of the three-quarter filled Peierls-Hubbard Hamiltonian. Various charge- and spin-ordered states are identified. In the strong-coupling regime, we find clear signatures of local lattice distortions accompanied by intrinsic multi-phonon localization. The results are discussed in relation to recent experiments on MX chain [-PtCl-] complexes. In particular we are able to reproduce the observed red shift of the overtone resonance Raman spectrum.

Keywords: charge density wave, localized lattice distortions, polarons, MX-chain compounds

Inspired by the recent observation of intrinsically localized vibrational modes in halide-bridged transition metal [-PtCl-] complexes [1], we study strong coupling effects between electronic and lattice degrees of freedom on the basis of a two-band, 3/4-filled Peierls-Hubbard model (PHM)

$$\mathcal{H} = -t \sum_{\langle i,j \rangle \sigma} c_{i\sigma}^\dagger c_{j\sigma} + \sum_{i\sigma} \varepsilon_i n_{i\sigma} + \sum_i U_i n_{i\uparrow} n_{i\downarrow} + \lambda_I (b_I + b_I^\dagger)(n_1 + n_3 - n_2 - n_4) + \hbar\omega_I b_I^\dagger b_I + \lambda_R (b_R + b_R^\dagger)(n_2 - n_4) + \hbar\omega_R b_R^\dagger b_R. \quad (1)$$

In (1), the $c_{i\sigma}^{[\dagger]}$ are fermion operators, $n_{i\sigma} = c_{i\sigma}^\dagger c_{i\sigma}$, and $b_R^{[\dagger]}$ and $b_I^{[\dagger]}$ are the boson operators for the Raman active (R) and infrared (I) optical phonon modes with bare phonon frequencies ω_R and ω_I . With regard to the quasi-1D charge density wave (CDW) system $\{\text{Pt(en)}_2[\text{Pt(en)}_2\text{Cl}_2](\text{ClO}_4)_4\}$ (en= ethylenediamine), subsequently abbreviated as PtCl, the Pt (Cl) atoms are denoted by the site index $i = 2, 4$ ($i = 1, 3$). The CDW state is built up by alternating nominal Pt^{+4} and Pt^{+2} sites with a corresponding distortion of Cl^- -ions towards Pt^{+4} . To model the situation of a 3/4-filled charge transfer insulator within a *single-mode approach* (SMA), we only include the R- (ν_1) -mode with $\hbar\omega_R = 0.05$ [2], and parametrize the site energies by $\Delta = (\varepsilon_{\text{Pt}} - \varepsilon_{\text{Cl}})/t = 1.2$ and the Hubbard repulsions by $U_{\text{Pt}} = 0.8$ and $U_{\text{Cl}} = 0$ (all ener-

gies are measured in units of t). Alternatively, we employ a more realistic *double-mode approach* (DMA), using $\hbar\omega_I = 0.06$ for the I- (ν_2) -mode [2].

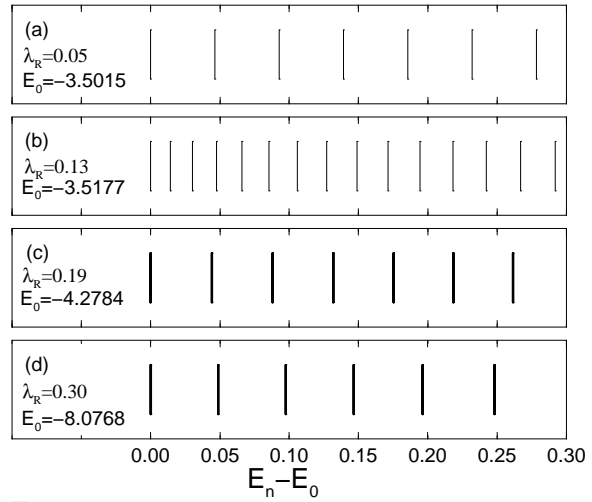


Figure 1: Low-energy part of the eigenvalue spectrum of the PHM [periodic boundary conditions, SMA]. Eigenvalues in (c) and (d) are two-fold degenerate.

The ground-state and spectral properties of the four-site PHM are determined by finite-lattice Lanczos diagonalization that preserves the full dynamics of the phonons [3].

Figure 1 shows the variation of the lowest energy states as a function of the electron-

Table 1: Relative red shift of the lowest-energy peaks in dependence on the final quanta of the vibrational energy [$\lambda_R = 0.19$; SMA].

r_n [%]	$n = 2$	3	4	5	5	7
Pt ³⁷ Cl [1]	0.4	1.1	2.4	4.6	7.7	11.6
SMA	0.4	1.3	2.8	4.8	7.5	10.9

Table 2: Different energy contributions to E_0 , local particle densities [$\langle n_i \rangle$], local magnetic moments [$L_i = 3\langle (n_{i\uparrow} - n_{i\downarrow})^2 \rangle / 4$], charge correlations [$\langle n_i n_j \rangle$] and magnetic structure factor [$S_s(\pi) = \frac{1}{N} \sum_{i,j} \langle S_i^z S_j^z \rangle e^{i\pi(i-j)}$] in the ground-state of the PHM. Note that the effect of Δ can be obtained dynamically within the DMA (see column 4).

	SMA		DMA	$\Delta = 0$
λ_I	0.0	0.0	0.15	0.15
λ_R	0.05	0.19	0.19	0.05
E_0	-3.5015	-4.2783	-5.3770	-3.2715
E_{kin}	-4.1115	-2.9186	-2.3202	-3.5985
E_{ph}	0.0001	2.1485	3.8490	0.2602
E_{el-ph}	-0.0036	-4.3026	-7.7017	-0.5433
E_U	0.6136	0.7945	0.7959	0.6102
$\langle n_{Cl} \rangle$	1.7047	1.8834	1.9561	1.7070
$\langle n_{Pt(2)} \rangle$	1.2953	0.2541	0.0949	1.2929
$\langle n_{Pt(4)} \rangle$	1.2953	1.9791	1.9929	1.2929
$\langle n_1 n_2 \rangle$	2.1053	0.3788	0.1441	2.1042
$\langle n_1 n_3 \rangle$	2.8611	3.5396	3.8253	2.8705
$\langle n_2 n_4 \rangle$	1.4990	0.4852	0.1824	1.4937
L_{Cl}	0.1897	0.0830	0.0323	0.1880
$L_{Pt(2)}$	0.3962	0.1696	0.0682	0.3977
$L_{Pt(4)}$	0.3962	0.0156	0.0053	0.3977
$S_s(\pi)$	0.1053	0.0524	0.0212	0.1042
Config.:	●-↑-●-↓	●-○-●-●	●-○-●-●	●-↑-●-↓

phonon coupling. In the weak-coupling region, the ground-state is basically a zero-phonon state (cf. Fig. 2 a) and the peaks in Fig. 1 (a) correspond to multiples of the fundamental phonon frequency $\omega_R^{(1)}$. As λ_R increases a strong mixing of electron and phonon degrees of freedom takes place, and finally the lowest states with total momentum $K = 0$ and $K = \pi$ become nearly degenerate. In this limit a non-linear lattice potential stabilizing

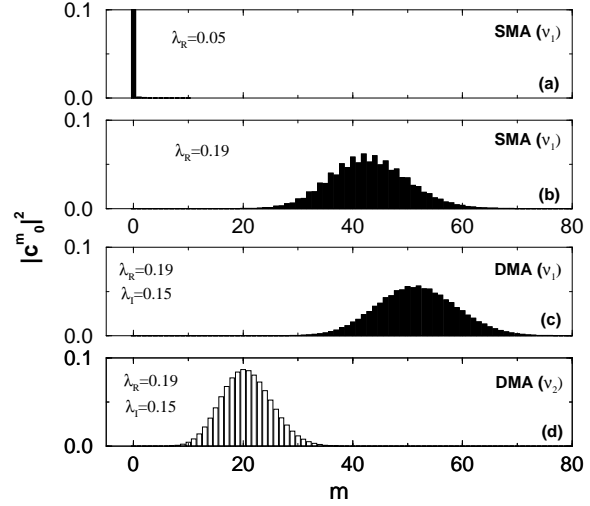


Figure 2: Phonon distribution in the ground state for the antisymmetric I (white columns) and symmetric Cl-Pt-Cl stretch R (black columns) phonon modes.

so-called *intrinsically localized vibrational modes* (ILMs) is self-consistently generated [1]. A prominent feature of these bound states is their strong anharmonic redshift, resulting from the attractive interaction of Raman phonon quanta located at the same PtCl₂ unit. The calculated red shift, $r_n = [n\omega_R^{(1)} - \omega_R^{(n)}] / \omega_R^{(1)}$ with $\omega_R^{(n)} = (E_n - E_0)$, of the (doublet) overtones shown in Fig. 1 (c) is successfully compared to experimental data probed by resonance Raman scattering (see Tab. 1). To elucidate the different nature of the ground state in the weak- and strong-coupling regimes, several characteristic quantities listed in Tab. 2. Obviously the self-localization transition is accompanied by significant changes in the spin- and charge correlations. As can be seen from the weight of the m -phonon state in the ground state, $|c_0^m|^2$ [3], depicted in Fig. 2, the appearance of the ●-○-●-● configuration is related to large occupation numbers of the localized vibrational (R) mode.

To summarize, the numerical results obtained for the PHM provide strong evidence for the existence of a dynamical spatial localization of vibrational energy (ILM) in MX solids, due to high intrinsic nonlinearity from strong electron lattice coupling.

- [1] B. I. Swanson et al., Phys. Rev. Lett. **82** (1999) 3288.
- [2] S. P. Love et al., Phys. Rev. B **47** (1993) 11107.
- [3] B. Bäuml et al., Phys. Rev. B **98** (1998) 3663.